Universal Journal of Fluid Mechanics 4 (2016), 29-41
www.papersciences.com

The Impact of DBD Plasma Actuator on Turbulent Characteristics in the Channel Flow: A Comparison between Two RANS Models

Amin Jafarimoghaddam[1] & Sadegh Aberoumand[2]
[1]Department of Aerospace Engineering, K. N. Toosi University of Technology, Tehran, Iran
a.jafarimoghaddam@gmail.com
[2]Department of Mechanical Engineering, Islamic Azad University, Takestan Branch, Takestan, Iran

Abstract
By the present study DBD plasma actuator was applied into a 2D incompressible channel flow to study turbulent structures by using a Finite Difference approach to k-ε turbulent model and also Realizable k-ε model. The actuator was simulated by Modified Lumped Circuit Element Electro-Static model just as the previous work [1]. The study was continued by Reynolds number of 5600 with constant inlet velocity profile. The length of the channel flow was considered to be long enough for reaching a fully-developed flow region. The results showed that Lorentz body force of the plasma actuator could reduce the fluctuation terms of velocity in general but since k-ε model is almost invalid near the walls especially where the strong velocity gradients by the actuator are dominant, a significant discrepancy was observed between the two turbulent models. Moreover, a hypothesis about the skin friction reduction by the DBD plasma jet actuator was discussed in this work. The features of the DBD plasma actuator were selected to be 2KV for the peak voltage amplitude, 10000 Hz for the voltage frequency and kapton as the dielectric in which the actuator can be considered as an almost weak Synthetic Jet Plasma generator.

Key Word and Phrases
DBD Plasma Based Channel Flow, Modified Lumped Circuit Element Electro-Static Model, Finite Difference approach to k-ε Turbulent Model, Realizable k-ε Model, The impact of Plasma Actuator on Turbulent Structures.

1. Introduction

Dielectric Barrier Discharge (DBD) plasma actuator had a variety of applications so far. It has been implemented as a device usually for flow reattachment, enhancing lift, decreasing drag (which is the main cause of fuel consumption [2]) and some other applications related to the nature of the plasma actuator. In order to control the behavior of the fluid flow, some models like moving objects, micro bubbles, hydrophobic surfaces, porous zones, corona plasma wind (applied by DC power supply) and DBD plasma actuator (applied by AC power supply) have been introduced so far [3]. Progress and development of DBD plasma actuators have been significant over the last two decades [4], [5]. Utilizing electric field for flow control has been reviewed by Cattefesta and Sheplak [6]. Plasma actuator has been tested in variety of applications [7]-[12] and it has been observed that the actuator causes a body force which is directed from the exposed electrode to the encapsulated one.

Because experimental investigations of plasma actuator are so expensive, CFD tools can be applied for discovering the nature of plasma actuator in different applications. Considering that, DBD plasma actuator works in a semi-steady mode, it can be inferred that it could be possible to decouple plasma equation from Navier- Stokes equations and then the solution of plasma is placed into Navier- Stokes equation as the source term. Since the different methodologies and models for solving the DBD plasma problem have been well discussed in the literature so far [13]- [15], so in the present research we have not focused on the methodology of solving the plasma problem. Then the goal of this investigation is to first compare a Finite Difference approach to k-ε turbulent model to Realizable k-ε model under a 2D incompressible flow regime in a one-sided DBD plasma based channel flow in order to study the behavior of fluctuation terms of velocities which are manipulated by the actuator. Since the skin friction coefficient (C_f) is governed by the wall shear stress and also

Reynolds stresses, by solving the laminar flow regime of plasma-based problems, we cannot proceed in predicting the behavior of skin friction coefficient. Wall shear stress is manipulated by the actuator in which rises strongly near the forcing region and then rapidly decreases. This rising in wall shear stress is a negative factor for skin friction reduction. Coming to this point that many studies have been presented by considering the impact of DBD plasma actuators under laminar flow regimes, the effect of Reynolds stresses has been almost neglected on skin friction drag so far for DBD plasma actuators. Then the main goal of this investigation is to numerically study the turbulent structures to see if they can behave effectively in friction drag reduction or not. Moreover, an implicit Finite Difference algorithm is introduced for discretizing and solving the k and ε equations of the turbulent models.

2. Modeling of DBD Plasma Actuator

In general, DBD plasma actuator can be modeled by Electro- Static Model. This model is specified in [1]. So, by the present work, we have only brought up the main governing equations.

Electrical potential is governed by the following Poisson equation [1]:

$$\nabla(\varepsilon\nabla\varphi) = \frac{1}{\lambda_D^2}\varphi \tag{2.1}$$

The charge density is obtained from the one- dimensional simulation of electric charge [1] as:

$$\rho_c = -\frac{\varepsilon_0}{\lambda_D^2}\varphi \tag{2.2}$$

By presenting the net charge in a region with the presence of electric field, the induced body force by the DBD plasma actuator can be calculated by:

$$\overrightarrow{f_b} = \rho_C \overrightarrow{E}. \tag{2.3}$$

2.1 Numerical Formulation of Modified Electro-Static Lumped Circuit Element Model

Generally, the model for DBD plasma actuator deals with solving (2.1) in a mathematical plain, obtaining induced body force due to the presence of the plasma actuator and then mapping the domain into the physical space of the problem. Since Lumped Circuit Element model, is an approach in which considers electrodes, air and dielectric as capacitor elements and each element as finite numbers of attached sectors (subscripted by n), then firstly, for modifying the Electro-Static model, the modified spatial-time Lumped Circuit Element model, discussed in [1], was used in order to obtain the region of the presence of plasma temporally, $x(t)$, and also dielectric virtual voltage $V_n(t)$ by simultaneously solving of eqs (2.4) to (2.6). Schematic of the model is shown in Fig.1.

$$\frac{dV_n(t)}{dt} = \frac{dV_{app}(t)}{dt}\left(\frac{C_{an}(t)}{C_{an}(t)+C_{dn}(t)}\right) + k_n \frac{I_{pn}(t)}{C_{an}(t)+C_{dn}(t)} \tag{2.4}$$

$$I_{pn}(t) = \frac{1}{R_n}[V_{app}(t) - V_n(t)] \tag{2.5}$$

$$\frac{dx(t)}{dt} = \nu v \left|V_{app}(t) - V_n(t)\right| \tag{2.6}$$

in which νv, is a coefficient representing the increase in the sweep velocity by the increase of applied voltage amplitude. νv is assumed to be $10\frac{m/s}{kV}$ in the present simulation. $V_{app}(t)$ represents the applied voltage amplitude, $V_n(t)$ is the voltage at the virtual electrode in

each sector of encapsulated electrode which is assumed to be on the surface of dielectric material, $I_{pn}(t)$ is the current through the plasma resistance for each sector, R_n is the air resistance in each section, C_{an} and C_{dn} are capacitor elements of air and dielectric respectively, and k_n is a constant which is assumed to be 0 or 1 depending on the presence of plasma in the last element.

Eqs (2.4) to (2.6) were solved by using second order Range-Kutta. Then, (2.1) was solved for spatial-time re-corrected conditions. Finally the obtained spatial steady body force was put into Navier- Stokes equations as the source term. Length of the exposed and encapsulated electrodes was assumed to be 0.5inch for both and also in the present work, vertical and horizontal distances between the electrodes were assumed to be 0.003 inch [1]. Based on the result of simulation by Electro- Static Model, plasma forms just on a region over the encapsulated electrode. This happens because there would be no assumption of the presence of charge density in other regions. Besides, it is noticeable that vertical body force is almost negligible in comparison with the horizontal body force. So, according to the results of the present simulation, the vertical term of the body force contains less than 8% of the horizontal body force. As the result of the present simulation by Lumped Circuit Element Electro-Static Model, the plasma body force is shown in Fig. 2.

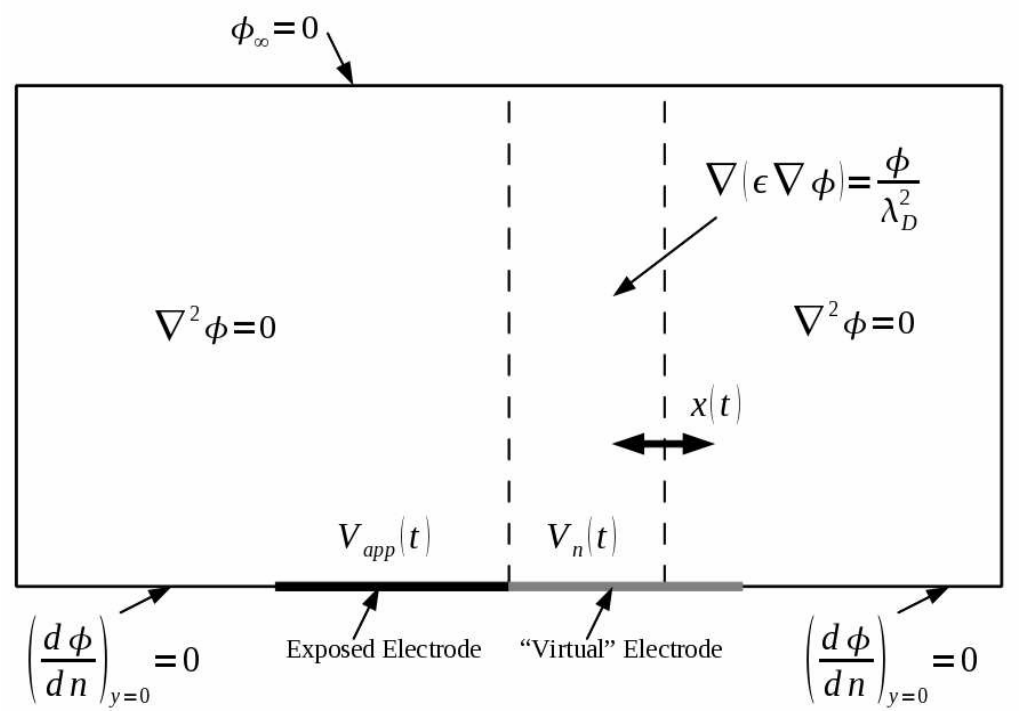

Fig.1 Governing Equations and Boundaries for the Modified Lumped Circuit Element Electro-Static Model [1]

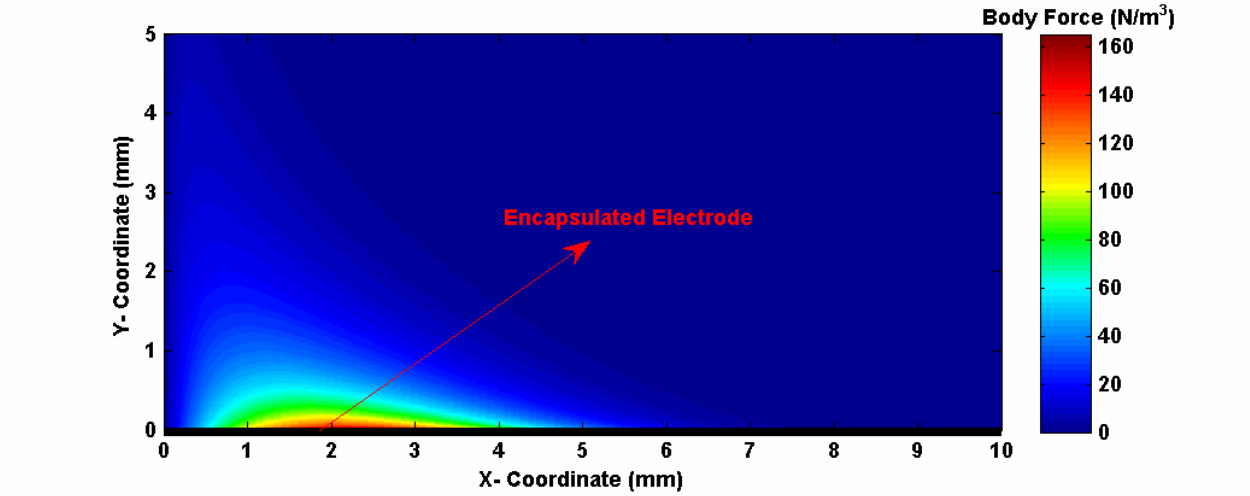

Fig. 2 Plasma body force for the actuator configuration of interest

3. Fluid Flow Equations

Coming to this point that fluid flow has been considered to be two dimensional and incompressible, in this work we used Vorticity- Stream Function numerical model for solving the fluid flow equations. By eliminating the pressure term from the momentum equations, the transport equation for Vorticity is obtained and also there will be one more Poisson equation left for the Stream Function variable from the continuity equation. If the steady spatial body force induced by the DBD plasma actuators is considered as a function of x and y (f(x, y)), the manipulated Transport and Poisson equations (RANS formation) can be obtained as:

$$\frac{\partial^2\psi}{\partial x^2}+\frac{\partial^2\psi}{\partial y^2}=-\xi$$

$$\rho\left(\frac{\partial\xi}{\partial t}+u\frac{\partial\xi}{\partial x}+v\frac{\partial\xi}{\partial y}\right)=(\mu+\mu_t)\left(\frac{\partial^2\xi}{\partial x^2}+\frac{\partial^2\xi}{\partial y^2}\right)+\frac{\partial f(x,y)}{\partial y}-\frac{\partial f(x,y)}{\partial x} \tag{3.2}$$

The above equations were discretized by using implicit FDM scheme (2016) [1].

4. Implementation of Finite Difference approach to k-ε & Realizable k-ε Turbulent Models

4.1 Finite Difference approach to k-ε

For k-ε turbulent model, transport equations of kinetic energy and energy dissipation can be given by eqs (4.1) and (4.2) respectively:

$$\frac{\partial(\rho k)}{\partial t}+div(\rho k\vec{U})=div\left[\frac{\mu_t}{\sigma_k}gtad(k)\right]+2\mu_t E_{ij}.E_{ij}-\rho\varepsilon \tag{4.1}$$

$$\frac{\partial(\rho\varepsilon)}{\partial t}+div(\rho\varepsilon\vec{U})=div\left[\frac{\mu_t}{\sigma_\varepsilon}gtad(\varepsilon)\right]+C_{1\varepsilon}\frac{\varepsilon}{k}2E_{ij}.E_{ij}-C_{2\varepsilon}\rho\frac{\varepsilon^2}{k} \tag{4.2}$$

where μ_t is the turbulent eddy- viscosity which supposed to represent the impact of unresolved velocity fluctuations of u', which is given by $\mu_t=C_\mu\rho\frac{k^2}{\varepsilon}$

E_{ij} , is the strain rate tensor in which for an incompressible flow can be denoted as:

$$E_{ij} = \frac{1}{2}\left(\frac{\partial u_i}{\partial x_j} + \frac{\partial u_j}{\partial x_i} \right). \tag{4.3}$$

The model consists of experimental constants which are described as follows:
$C_\mu = 0.09,\ \sigma_k = 1.0,\ \sigma_\varepsilon = 1.3,\ C_{1\varepsilon} = 1.44$ and $C_{2\varepsilon} = 1.92$.

For the present work, we assumed the axillary parameter of $\lambda = \frac{\varepsilon}{k}$, to decouple the transport equations.

By considering $P_k = \frac{\mu_t}{2}(\frac{\partial u}{\partial y} + \frac{\partial v}{\partial x})^2$, the transport equations of k and ε for an incompressible flow can be rewritten as:

$$\frac{\partial k}{\partial t} + \nabla.(k\vec{U} - \frac{\nu_t}{\sigma_k}\nabla k) + \lambda k = P_k \tag{4.4}$$

$$\frac{\partial \varepsilon}{\partial t} + \nabla.(\varepsilon\vec{U} - \frac{\nu_t}{\sigma_\varepsilon}\nabla \varepsilon) + C_{2\varepsilon}\lambda\varepsilon = C_{1\lambda}P_k \tag{4.5}$$

Utilizing Finite Difference method by an Alternative Directional Implicit (ADI) scheme for 2D incompressible flows, the final algebraic form can be achieved by the following eqs (4.6) to (4.9):

For K transport equation, the sweep procedure in X- Direction of the channel flow can be written as:

$$(B\frac{\Delta t}{2})k^{\frac{n+1}{2}}(i-1,j) + ((A+\lambda)\frac{\Delta t}{2}+1)k^{\frac{n+1}{2}}(i,j) - B\frac{\Delta t}{2}k^{\frac{n+1}{2}}(i-1,j) = k^n(i,j) + \frac{\Delta t}{2}Ck^n(i,j+1) - Ck^n(i,j-1) + \frac{\Delta t}{2}P_k \tag{4.6}$$

For K transport equation, the sweep procedure in Y- Direction of the channel flow can be written as:

$$(C\frac{\Delta t}{2})k^{n+1}(i,j-1) + ((A+\lambda)\frac{\Delta t}{2}+1)k^{n+1}(i,j) - C\frac{\Delta t}{2}k^{n+1}(i,j+1) = k^{\frac{n+1}{2}}(i,j) + \frac{\Delta t}{2}Bk^{\frac{n+1}{2}}(i+1,j) - Bk^{\frac{n+1}{2}}(i-1,j) + \frac{\Delta t}{2}P_k \tag{4.7}$$

The same routine could be pursued for ε transport equation, and then the sweep procedure in X-Direction of the channel flow can be written as:

$$(B\frac{\Delta t}{2})\varepsilon^{\frac{n+1}{2}}(i-1,j) + ([A'+C_{2\varepsilon}\lambda]\frac{\Delta t}{2}+1)\varepsilon^{\frac{n+1}{2}}(i,j) - B\frac{\Delta t}{2}\varepsilon^{\frac{n+1}{2}}(i-1,j) = \varepsilon^n(i,j) + \frac{\Delta t}{2}C\varepsilon^n(i,j+1) - C\varepsilon^n(i,j-1) + \frac{\Delta t}{2}C_{1\varepsilon}\lambda P_k \tag{4.8}$$

And finally for ε transport equation, the sweep procedure in Y- Direction of the channel flow can be written as:

$$(C\frac{\Delta t}{2})\varepsilon^{n+1}(i,j-1) + ([A'+C_{2\varepsilon}\lambda]\frac{\Delta t}{2}+1)\varepsilon^{n+1}(i,j) - C\frac{\Delta t}{2}\varepsilon^{n+1}(i,j+1) = \varepsilon^{\frac{n+1}{2}}(i,j) + \frac{\Delta t}{2}B\varepsilon^{\frac{n+1}{2}}(i+1,j) - B\varepsilon^{\frac{n+1}{2}}(i-1,j) + \frac{\Delta t}{2}C_{1\varepsilon}\lambda P_k \tag{4.9}$$

In eqs (4.10) to (4.13), the factors of A, A',B and C are defined as follows:

$$A=2\frac{\mu_t}{\sigma_k}\left(\frac{1}{\Delta x^2}+\frac{1}{\Delta y^2}\right) \tag{4.10}$$

$$A'=2\frac{\mu_t}{\sigma_\varepsilon}\left(\frac{1}{\Delta x^2}+\frac{1}{\Delta y^2}\right) \tag{4.11}$$

$$B=\frac{-u}{2\Delta x}+\frac{\nu_t}{\Delta x^2} \tag{4.12}$$

$$C=\frac{-v}{2\Delta y}+\frac{\nu_t}{\Delta y^2} \tag{4.13}$$

where u and v are the solved velocities in X and Y directions respectively. Eqs (4.6) to (4.9) are solved by using TDMA algorithm while in each time step, the values of λ and μ_t must be updated. To update eddy viscosity and auxiliary parameter of λ, the following procedure was pursued as discussed in [16]. Since eddy viscosity is limited by a certain fraction of molecular viscosity near the walls and its maximum value of $\nu_{t\max}=l_{\max}\sqrt{k}$ (where $l_{\max}$ is the maximum certifiable mixing length, which represents the largest size of eddies that can be considered as the width of the domain), the limited mixing length can be defined as $l_l=C_\mu\frac{k^{1.5}}{\varepsilon}$ if $C_\mu k^{1.5}<\varepsilon l_{\max}$ or $l_{\max}$ if otherwise. Then eddy viscosity can be quantified as $\nu_t=\max(\nu_{t\min},l_l\sqrt{k})$ and finally, the auxiliary parameter of λ is updated to $\lambda=C_\mu\frac{k}{\nu_t}$.

4.2 Boundary Conditions for k-ε Turbulent Model

For inlet condition, the value for k and ε can be assumed to be:

$$k=\xi U_\infty{}^2 \tag{4.14}$$

$$\varepsilon=\frac{k^{\frac{3}{2}}}{0.1\delta} \tag{4.15}$$

where ξ is a constant that is assumed to be 0.01 in the present work and δ is the half of the modeled channel flow.

For walls conditions, the value for k and ε is assumed to be:

$$k=0 \tag{4.16}$$

$$\varepsilon=2\nu\frac{d}{dy}\sqrt{k} \tag{4.17}$$

For outlet condition, the value for k and ε is calculated by the following Dirichlet boundary conditions:

$$\frac{\partial k}{\partial x}=0 \tag{4.18}$$

$$\frac{\partial \varepsilon}{\partial x}=0 \tag{4.19}$$

4.3 Realizable k-ε Model

In order to improve the compatibility of k-ε turbulent model, we have modified the previous form of transport equations by Realizable scheme of k-ε model in which k-transport equation remains unchanged but transport equation of ε obtains some modifications. Having variable value for C_μ instead of a constant, would let the Realizable form predict the curved stream lines in a much better way. The modifications can easily follow the previous scheme of discretization for k-ε model; so in this study, we have only presented the transport equations and illustrated the differences between the two turbulent models. It is noticeable that other constants of k-ε model are also different in Realizable form of k-ε model.

The equation for k and ε are as follows:

$$\frac{\partial(\rho k)}{\partial t}+\frac{\partial(\rho u_j k)}{\partial x_i})=\frac{\partial}{\partial x_i}\left[(\mu+\frac{\mu_t}{\sigma_t})\frac{\partial k}{\partial x_j}\right]+\mu_t S^2-\rho\varepsilon \tag{4.20}$$

$$\frac{\partial(\rho\varepsilon)}{\partial t}+\frac{\partial(\rho u_j \varepsilon)}{\partial x_i})=\frac{\partial}{\partial x_i}\left[(\mu+\frac{\mu_t}{\sigma_\varepsilon})\frac{\partial \varepsilon}{\partial x_j}\right]+\rho C_1 S\,\varepsilon+\rho C_2\frac{\varepsilon^2}{k+\sqrt{\nu\varepsilon k}} \tag{4.21}$$

in which $C_1=\max\left\{0.43,\frac{\eta}{\eta+5}\right\}$ $\eta=S\frac{k}{\varepsilon}$ $S=\sqrt{2S_{ij}.S_{ij}}$

The constant in the model are defined as:
$C_{1\varepsilon}=1.44$, $C_2=0.9$, $\sigma_k=1$ and $\sigma_\varepsilon=1.2$.

For achieving the variable C_μ, the following expression must also be updated in each time step.

$$C_\mu=\frac{1}{A_0+A_S\frac{kU^*}{\varepsilon}} \tag{4.22}$$

In expression (4.22), A_0, A_S and U^* are functions of strain rate tensor and angular velocity. Realizable form of k-ε model can be easily discretized as the same as its standard form. Noting that linearization parameter of λ can convert the nonlinear term of (4.21) into a linear one.

5. Numerical Results and Discussions

For the plasma configuration of interest, and the inlet Reynolds number of 5600, k-ε and Realizable k-ε turbulent models were implemented to capture fluctuation characteristics of the velocity in the plasma based channel flow. The geometry of the problem is drawn in Fig. 3.

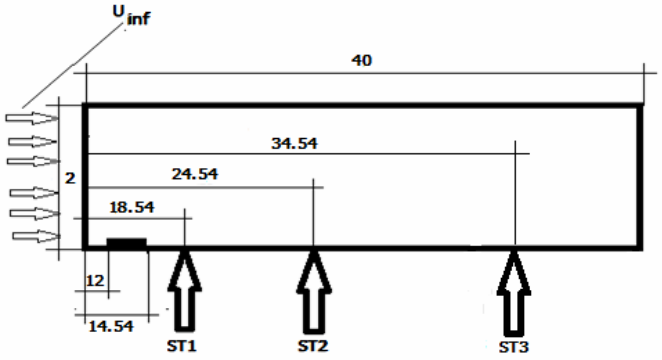

Fig.3 Schematic of the problem (distances are in the scale of centimeter)

The problem is a physical domain which tracks the flow from a uniform inlet velocity to some further to the location that the flow is fully-developed in which the location of ST3 is selected in a distance far enough from the inlet where the flow was completely fully-developed. The channel flow without plasma actuator was solved to validate the codes by a previous work by Kim et.al [17] and the results are shown in Figs 4 to 6. Figs 7 and 8 show the velocity profiles in the three selected locations for each studied case (with and without plasma). In order to compare the two turbulent models, normalized fluctuation characteristics of u_{rms}, v_{rms} and $\overline{u'v'}$ (for the two RANS models in the case of using plasma) are compared with case of without using plasma. The results are shown in Figs 9 to 11. According to the simulation results, the plasma strength is obscured by passing through the channel flow. It is obviously shown that the plasma actuator can behave as a damper which tends to turn the turbulent regime to a laminar one by diminishing the fluctuation terms in general. The almost mesh-independent solution for k-ε models was obtained on using 480,000 grids for the computational domain. The distance from the bottom wall to the nearest internal grid corresponded to $y+ \approx 0.69$ and $y+ \approx 0.62$ for standard k-ε and Realizable k-ε models respectively.

According to the results of the two turbulent models, by using k-ε turbulent model, fluctuation terms were almost increased just near the bottom wall where the strong gradients of velocity by the plasma actuator are dominant and then returns to the values almost lower than the base line flows. Two effects are common for the failure of k-ε model near the wall and to make it almost invalid. Firstly, the greater velocity gradients occur near the wall where the viscos flow dominates and in the case of using plasma, there would be much stronger velocity gradients on this region and considering that k-ε model suffers from predicting curved stream lines caused by strong velocity gradients, its failure is anticipated. Secondly, by having lower inlet Reynolds numbers, molecular viscosity is more considerable than the eddy-viscosity near the walls and subsequently the model requires some modifications [16], but in the present study, by selecting 5600 as the inlet Reynolds number, this effect is almost ignorable. This can be seen from the results of k-ε models in the case of without plasma which has a good agreement with the study by Kim et.al [17].

Noting that Realizable k-ε is a stronger model than its standard model, we can take the advantage of Realizable k-ε results as the failure of standard k-ε model in predicting the turbulent structures in a one- sided DBD plasma based channel flow. According to the Realizable k-ε results, DBD plasma actuators can almost turn the turbulent flow regime to the laminar for any region near the wall. Besides, standard k-ε model cannot diminish the fluctuation terms just after the wall. The simulation showed that the mean reduction of fluctuation terms for Reynolds stresses (measured from the bottom wall to Y+ of 50 from the inlet to the fully- developed location) was about 11.5% and 36.2% for standard k-ε and Realizable k-ε models respectively. This can be considered as a significant error for standard k-ε turbulent model with the presence of plasma body force.

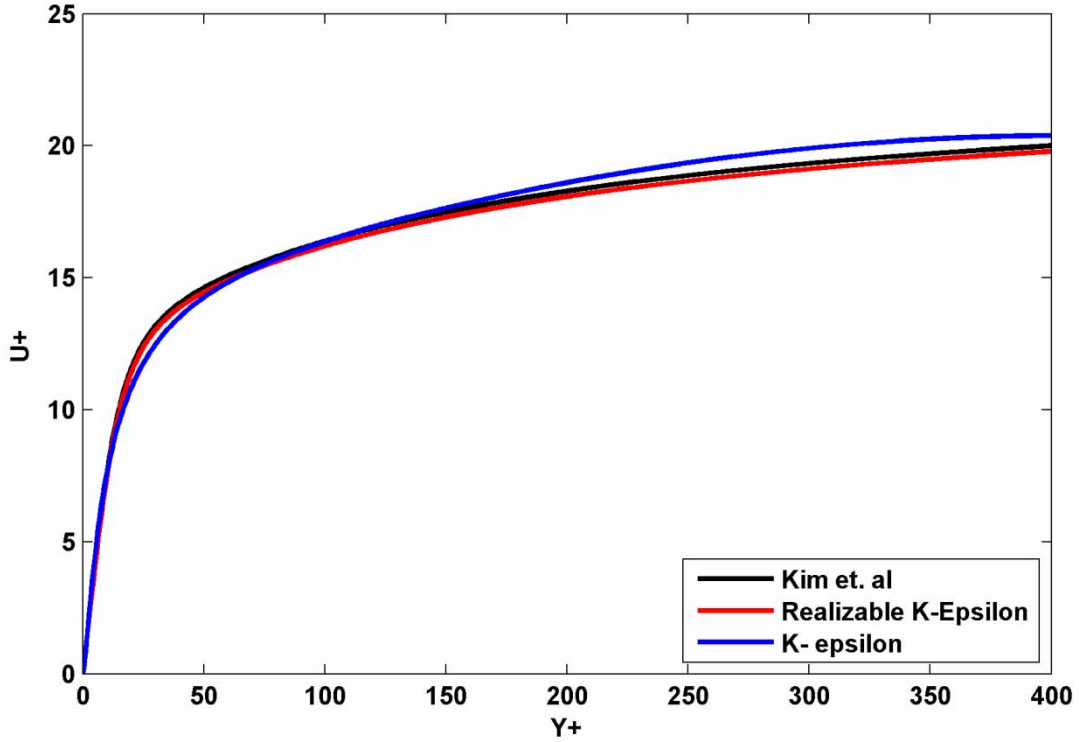

Fig.4 Comparison between u^+ of the two turbulent models without using plasma for fully-developed location and the report by Kim el.al [17]

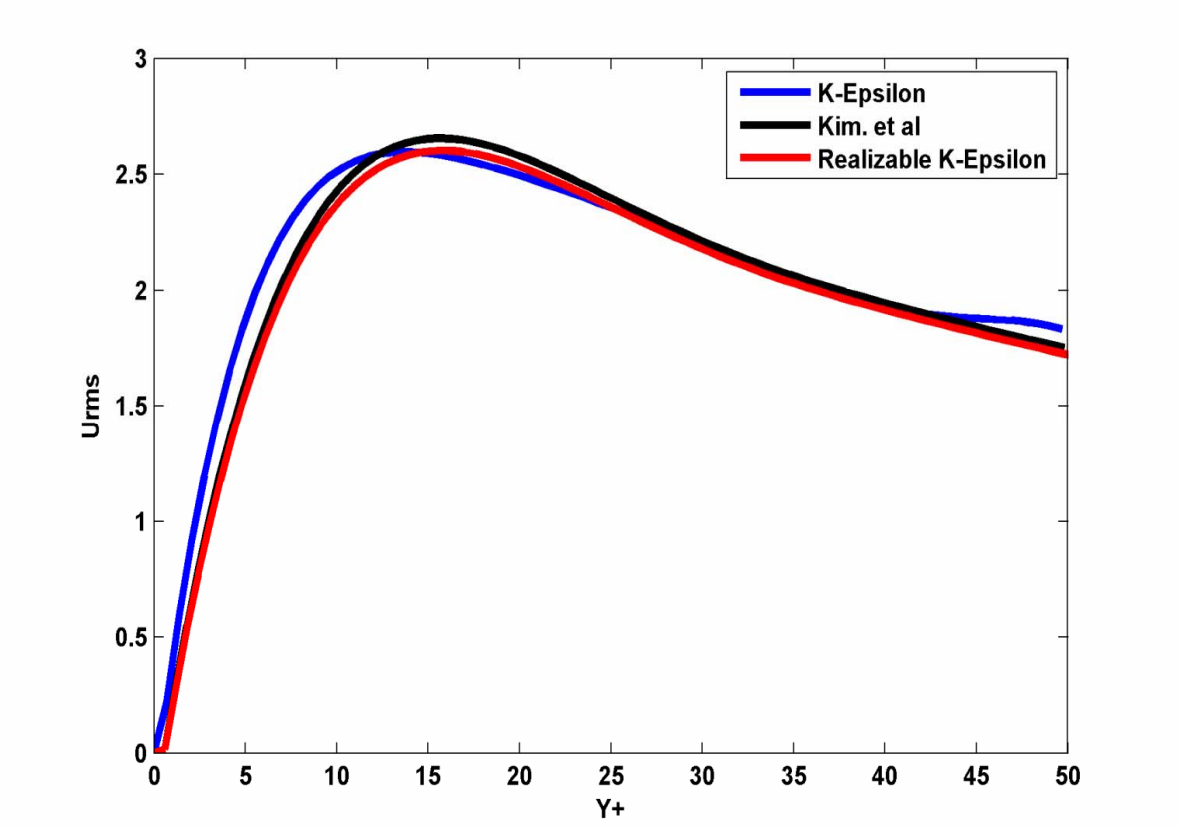

Fig. 5 Comparison between normalized u_{rms} of the two turbulent models without using plasma for fully- developed location and the report by Kim el.al [17]

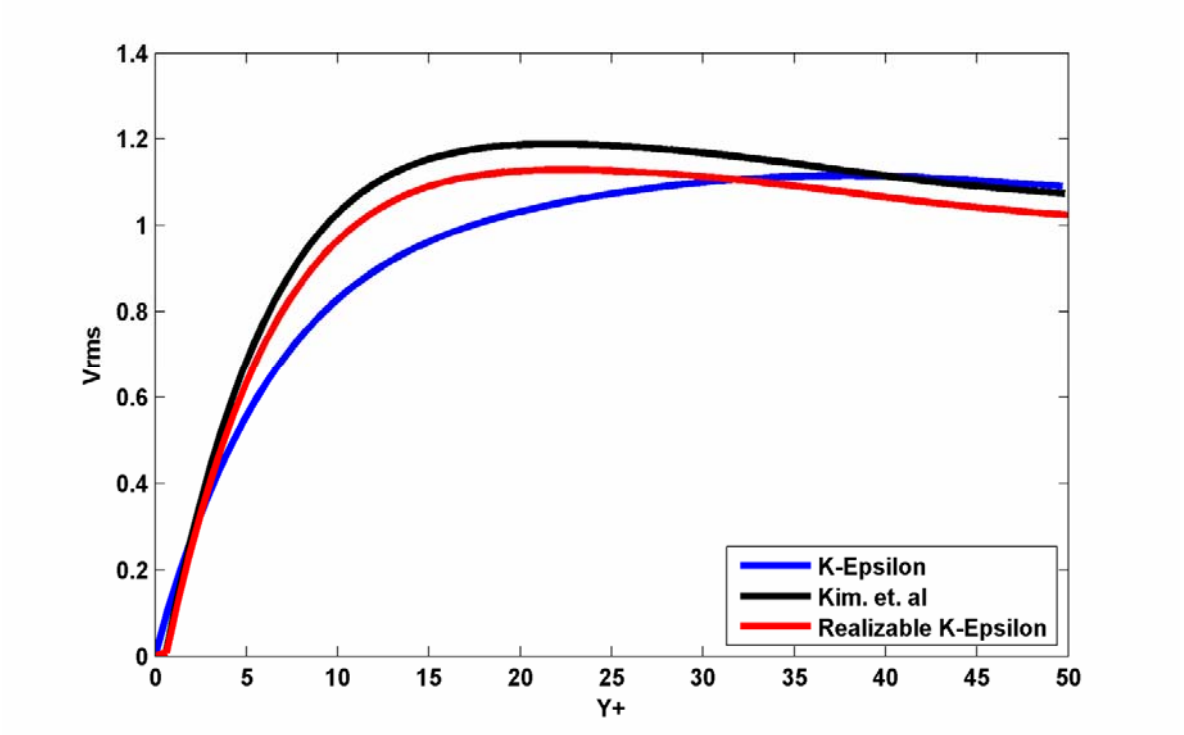

Fig. 6 Comparison between normalized v_{rms} of the two turbulent models without using plasma for fully- developed location and the report by Kim el.al [17]

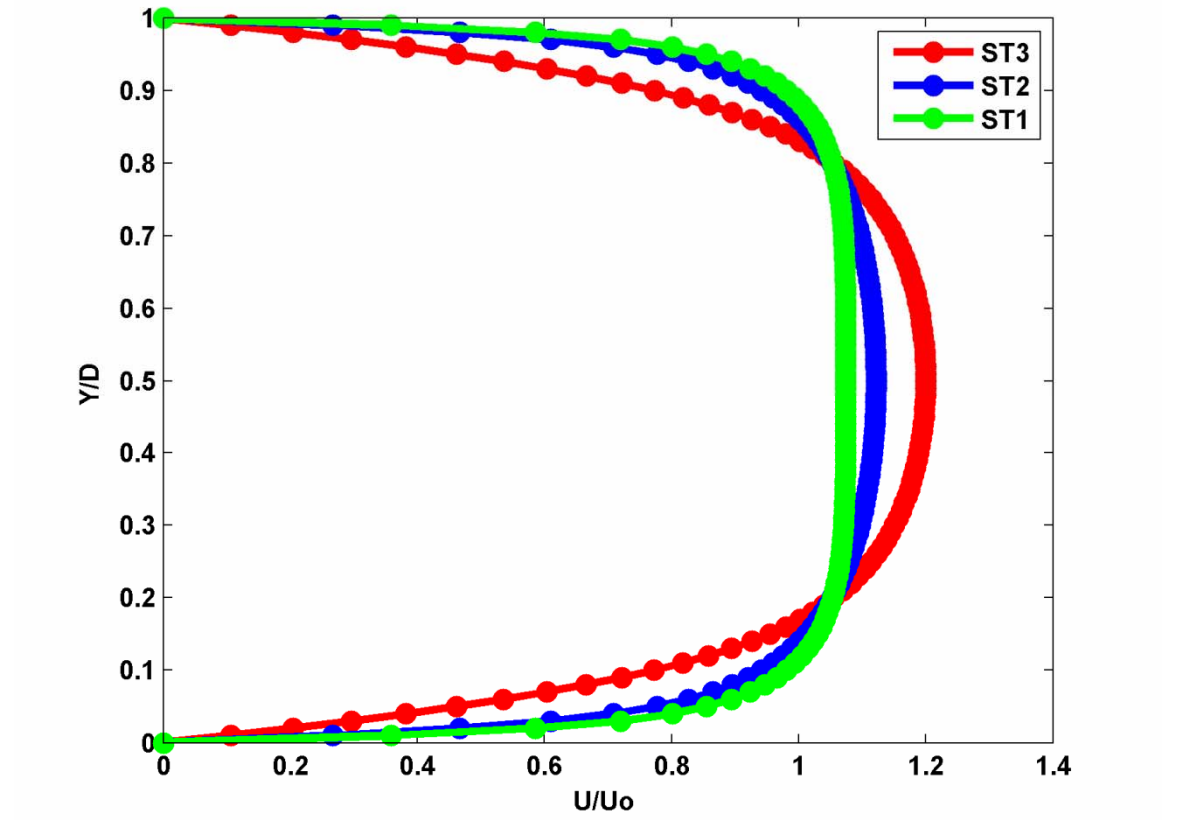

Fig.7 Velocity profile in three selected locations of the channel flow without plasma, by Realizable k-ε model (the results by k-ε model were accurately the same in this case)

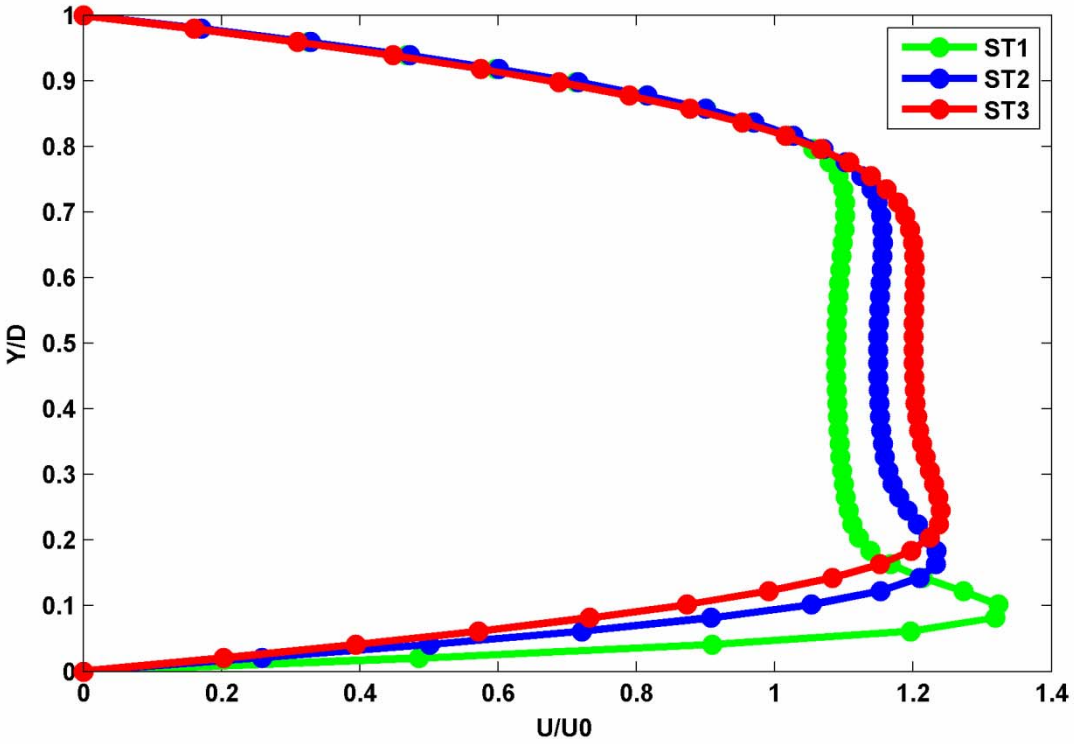

Fig. 8 Velocity profile three selected locations of the channel flow with plasma, by Realizable k-ε model (the results by k-ε model were accurately the same in this case)

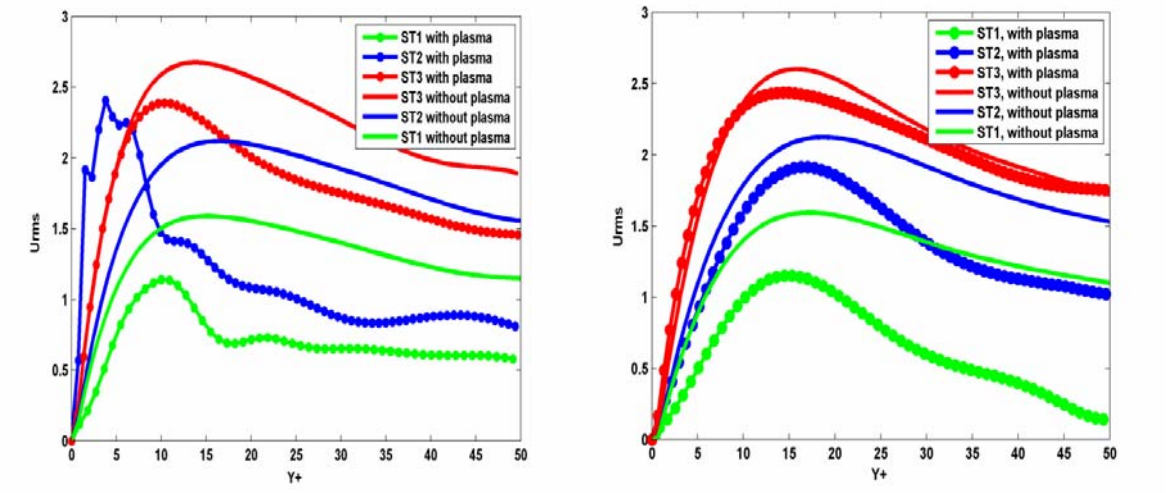

Fig. 9 Normalized u_{rms} in three selected locations of the problem (Realizable k-ε model (left) , standard k-ε turbulent model (right))

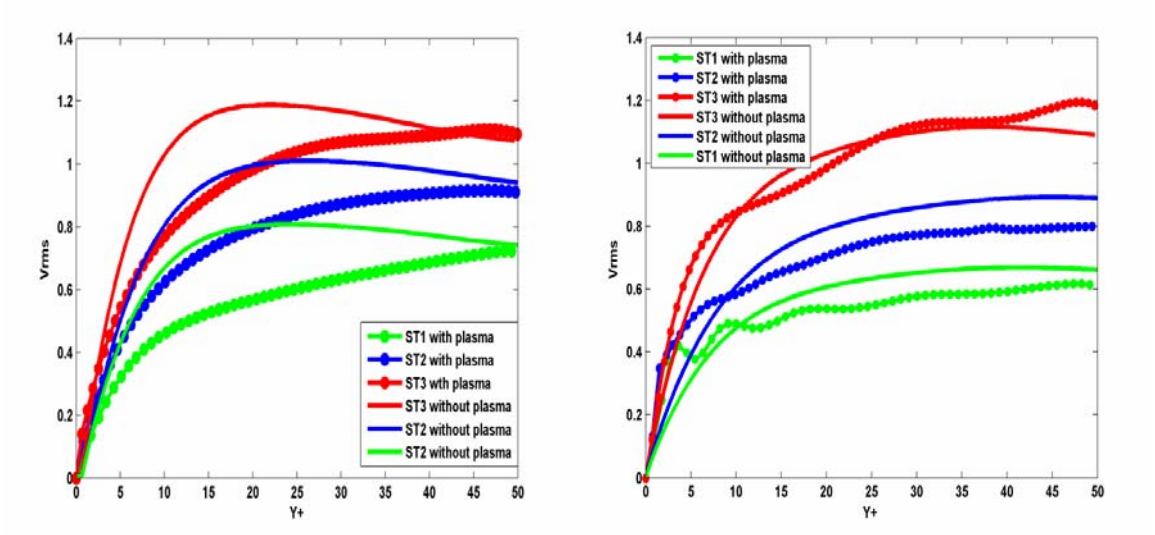

Fig. 10 Normalized v_{rms} in three selected locations of the problem (Realizable k-ε model (left), standard k-ε turbulent model (right))

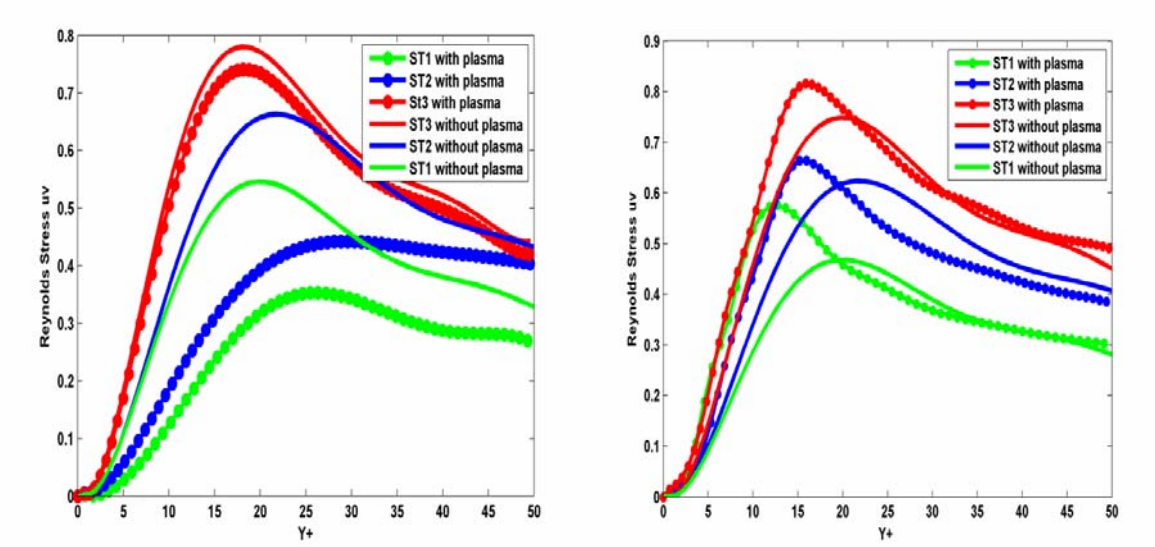

Fig. 11 Normalized $\overline{u'v'}$ in three selected locations of the problem (Realizable k-ε model (left), standard k-ε turbulent model (right))

6. Conclusions

By the present research, the impact of DBD plasma jet actuator with the configuration of 2kV for the peak voltage amplitude, 10000 Hz for the voltage frequency, Kapton for the dielectric material and the length of exposed and encapsulated electrodes of 0.5inch, was numerically studied in the channel flow under an incompressible turbulent flow regime by an Implicit Finite Difference approach to k-ε turbulent model and also Realizable k-ε model for the inlet Reynolds number of 5600. Two aims have been followed during this study. Firstly, was to compare k-ε model to Realizable k-ε. And we found that for standard k-ε model, despite having acceptable results in a channel flow without using plasma jet actuator, the results were significantly fault when the actuator is applied; especially just near the bottom wall which was discussed in the previous section of this work.

Secondly, according to the Realizable k-ε results, DBD plasma actuator can almost convert the turbulent behavior to the laminar one, which was shown in this work as the manipulation of fluctuation terms. Fluctuation terms of velocity reduced with the average of about 11.5% and 36.2% for standard k-ε and Realizable k-ε models respectively (measured from the bottom wall to Y+ of 50 from the inlet to the location of ST3 in which the flow is fully developed without using plasma actuator). This reduction in Reynolds stresses is a significant factor which can act in the opposite of velocity gradients effect near the wall on the skin friction coefficient. Then there is a hypothesis about the contribution of these two main effects on skin friction reduction. This hypothesis will be examined in detail in further research.

Acknowledgements
Authors would like to thank for the great helps of Dr. Mani Fathali in fulfilling the present research.

References:

1. *Aberoumand, S., Jafarimoghaddam, A. and Aberoumand, H.,* 'Numerical Investigation on the Impact of DBD Plasma Actuators on Temperature Enhancement in the Channel Flow', *Heat Trans. Asian Res.. doi: 10.1002/htj.21227, (2016)*
2. *Gad-el-Hak M., 'Flow Control: Passive, Active, and Reactive Flow Management',* 1st ed,. Virginia Commonwealth University, Cambridge University Press, Cambridge, *2000.*
3. *Braun E.M., Lu F.K., Wilson D.R..,* 'Experimental research in aerodynamic control with electric and electromagnetic fields', *Progr. Aerosp. Scien., **45** (2009), 30-49.*
4. *Corke T.C., Enloe C.L., Wilkinson S.P.,*'Dielectric barrier discharge plasma actuators for flow control Annual Review of Fluid Mechanics', ***42** (2010),:505-529.*
5. *Moreau E.,* 'Airflow control by non-thermal plasma actuators', *J Phys D: Appl Phys., **40** (2007), 605-636.*
6. *Cattafesta L.N., Sheplak M.,* 'Actuators for Active Flow Control', *Ann. Rev. Fluid Mech., **43** (2011), 247-272.*
7. *Zhang P.F., Wang J.J., Feng L.H., Wang G.B.,*'Experimental study of plasma flow control on highly swept delta wing', *AIAA J., **48** (2010), 249-252.*
8. *Sosa R., Arnaud E., Memin E., Artana G.,* 'Study of the flow induced by a sliding discharge', *IEEE Trans. Dielectrics Electrical Insul.,**16** (2009), 305-311.*
9. *Orlov D.M., 'Modelling and Simulation Of Single Dielectric Barrier Discharge Plasma Actuators [Dissertation]'.* Notre Dame, Indiana: University of Notre Dame, *2006.*
10. *Orlov D.M., Apker T., He C., Othman H., Corke T.C.,* 'Modeling and Experiment of Leading Edge Separation Using SDBD Plasma Actuators', *AIAA Paper No 2007-087, (2007), 1-18.*
11. *Corke T.C., Post M.L., Orlov D.M.,* 'Single Dielectric Barrier Discharge Plasma Enhanced Aerodynamics: Concepts, Optimization and Applications', *J Propul Power, **24** (2008), 935-945.*
12. *Corke T.C., Post M.L., Orlov D.M.,* 'Single Dielectric Barrier Discharge Plasma Enhanced Aerodynamics: Physics, Modeling and Applications', *(Review Article), Exper. Fluids, (2009),1-44.*
13. *Ibrahim I..H., Skote M.,* 'Simulating plasma actuators in a channel flow configuration by utilizing the modified Suzen–Huang model', *Comp. Fluids, **99** (2014), 144–155.*
14. *Suzen Y. B., Huang P. G., Ashpis D. E.,* 'Numerical Simulations of Flow Separation Control in Low-Pressure Turbines using Plasma Actuators', *45th AIAA Aerospace Sciences Meeting and Exhibit, 8 - 11 January 2007, Reno, Nevada.*
15. *Kelsey Thomas, West I.V.,'Numerical investigation of plasma actuator configurations for flow separation control at multiple angles of attack',* Master Thesis, Missouri University of Science and Technology, *2012.*
16. *Lew A. J., Buscaglia G.C., Carrica P.M.,* 'A Note on the Numerical Treatment of the k-epsilon Turbulence Model', *Int. J. Comp. Fluid Dyn., **14** (2001), 201–209.*
17. *Kim J., Moin P., Moser R.,*"Turbulence statistics in fully developed channel flow at low Reynolds number', *NASA Ames Research Center, Moffett Field, CA 94035, USA.*